

Guide to answers for written examination in TSBB09 Image Sensors, 2021-01-11

Maria Magnusson, maria.magnusson@liu.se

PART I: STANDARD CAMERAS & IR SENSORS

Exercise 1

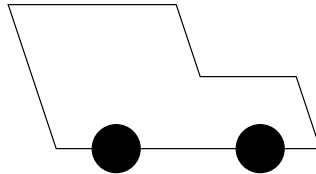
At a point $\mathbf{x} = (x_1, x_2, x_3)$ in space we can measure how much light energy that travels in the direction $\hat{\mathbf{n}} = (n_1, n_2, n_3)$.

Exercise 2

The phenomena is called vignetting or the \cos^4 -law. There is an attenuation of the image towards the edges of the image, approximately according to \cos^4 .

Exercise 3

In a rolling shutter camera, each successive line is exposed at successive points in time. Suppose that the image is exposed from top to bottom. Then the image would look approximately as shown below.



Exercise 4

Along sharp edges, there are high frequencies. Often bilinear interpolation is utilized for the conversion from Bayer images to RGB images. Then there is a risk for artifacts caused by aliasing. More advanced interpolation can mitigate these artefacts.

Exercise 5

The reason is that there is heat within the camera.

Exercise 6

To measure a correct temperature, the emissivity must be known and the camera must be set accordingly. The emissivity of human skin is high (0.98), whereas the emissivity of aluminum is lower (e.g. 0.11-0.31 for oxidized aluminum).

Exercise 7

- a) In CCD, charges are shifted out row by row and column by column from the sensor chip, i.e., all of the image needs to be transferred to circuits where charges are converted to voltage and then to a binary representation. In a CMOS camera each individual detector can be connected to a row and column readout line, similar to a RAM memory, from which conversion to a binary representation is done. This makes it possible to read out smaller parts of the image, but at a higher rate in time compared to a whole image.
- b) Due to the long readout line, from the detector to the conversion stage, the basic CMOS has higher noise levels than CCD. By using additional transistors at each detector element (APS), the CMOS design can be improved in terms of noise.

Exercise 8

- a) In the focal plane, the PSF is $\text{sinc}(u)0.5\text{sinc}(0.5u)$.
- b) Here, the image is certainly out-of-focus. The out-of-focus PSF takes the shape of a scaled version the camera aperture.

PART II: GEOMETRY AND MULTIPLE VIEWS**Exercise 9**

$$f(r) = r^2, g(r) = r^4, h(r) = r^6$$

Exercise 10

Tangential distortion occurs when the lens and the sensor plane are not parallel. (The tangential distortion coefficients p_1 and p_2 model this type of distortion.)

Exercise 11

$$\mathbf{A}_1 = \begin{pmatrix} 550 & 0 & 190 \\ 0 & 450 & 134 \\ 0 & 0 & 1 \end{pmatrix}.$$

Exercise 12 Let k be a constant. Then

$$\mathbf{H} = \begin{pmatrix} k \cdot H_{11} & k \cdot H_{12} & k \cdot H_{13} \\ k \cdot H_{21} & k \cdot H_{22} & k \cdot H_{23} \\ k \cdot H_{31} & k \cdot H_{32} & k \end{pmatrix}$$

describes exactly the same homography.

Exercise 13

$$(x_s, y_s, z_s) = (x_n, y_n, 1) / \sqrt{x_n^2 + y_n^2 + 1}$$

Exercise 14

Use a blending weight function **alpha** that has smaller values at the edges of the image and larger values at the center. **Pano1** and **Pano2** are the two images transformed to the reference grid. **alpha1** and **alpha2** are the weight image (**alpha**) transformed to the reference grid. Perform normalized weighting:

$$\text{Pano} = \frac{\text{alpha1} \cdot \text{Pano1} + \text{alpha2} \cdot \text{Pano2}}{\text{alpha1} + \text{alpha2}}$$

This way the borders of the individual images will be invisible in the panorama.

Exercise 15

See the figure in the exam. The point $p_i = (0, p_{iy}, f)^T$ and $p_r = (u_0, v_0 + h/2)^T$. Therefore

$$s \begin{pmatrix} u_0 \\ v_0 + h/2 \\ 1 \end{pmatrix} = \begin{pmatrix} \alpha & 0 & u_0 \\ 0 & \beta & v_0 \\ 0 & 0 & 1 \end{pmatrix} \begin{pmatrix} 0 \\ p_{iy} \\ f \end{pmatrix}. \quad (1)$$

The second row gives $s(v_0 + h/2) = \beta p_{iy} + v_0 f$ and the third row gives $s = f$. Therefore $f(v_0 + h/2) = \beta p_{iy} + v_0 f$, which gives $p_{iy} = fh/(2\beta)$.

Finally, $\phi_{\text{FOV}} = 2 \arctan(p_{iy}/f) = 2 \arctan(h/(2\beta)) = \arctan(360/(2 \cdot 700)) = 0.2517 = 14.4^\circ$.

Exercise 16

One measurement with a calibration plane gives one homography

$$\mathbf{H} = \mathbf{A}[\mathbf{R} \ \mathbf{t}].$$

The \mathbf{H} matrix gives $k_1 = 8$ new parameters, but $k_2 = 3$ parameters is needed to determine \mathbf{R} and $k_3 = 3$ parameters is needed to determine \mathbf{t} . Consequently only $k_1 - k_2 - k_3 = 8 - 3 - 3 = 2$ parameters is left to determine \mathbf{A} .

- a) Three measurement with the calibration plane gives $3 \cdot 2 = 6$ parameters to determine \mathbf{A} . This is enough since there are 5 unknowns in \mathcal{A} . Consequently, the minimum number of calibration planes is 3.
- b) Two measurement with the calibration plane gives $2 \cdot 2 = 4$ parameters to determine \mathbf{A} . This is enough since there are 4 unknowns in \mathcal{A} . Consequently, the minimum number of calibration planes is 2.

PART III: NON-STANDARD IMAGE SENSORS

Exercise 17

The center of the detector is in focus if the lens-law $1/f = 1/a_0 + 1/b_0$ is fulfilled. When $a_0 \tan \beta = b_0 \tan \alpha$ (Scheimpflugs condition) is fulfilled, the whole sensor is in perfect focus. Combining the two equations gives $\tan \beta = (b_0/f - 1) \cdot \tan \alpha = (17.5/17 - 1) \cdot \tan(60\pi/180)$, which gives that the sensor should be tilted $\beta = 0.0509 = 2.9^\circ$.

Exercise 18

For time-of-flight, occlusion do not occur.

For laser triangulation, both laser and camera occlusion may occur.

Exercise 19

The program below calculates a maximum intensity projection (MIP) image, $M(x, z)$.

```
for z=-127 to 128
  for x=-127 to 128
    M(x,z):=0;
    y:=-127;
    do
      if (M(x,z)<f(x,y,z)) M(x,z):=f(x,y,z);
      y:=y+1;
    while (y<129)
  end;
end;
```

Exercise 20

For a push-broom camera, the aperture is a line and the columns of the image are sampled at different time points. For a pin-hole camera, the aperture is a point and the whole image is sampled at the same time point.

Exercise 21

f_k looks like a scaled version of the (approximate) aperture pattern. The size (scale) of f_k varies with k , which is proportional to the depth.

Exercise 22

The point-spread function becomes independent on the distance to the object. Then, deblurring, i.e. to make the image sharp, can be done with only one fix filter. This filter does not depend on the depth as in the previous exercise.

Exercise 23

- a) For white light, $\mathbf{I} = [1, 1, 1]$. Set
 $\mathbf{M}_a = [0.25, 0.20, 0.07]$,
 $\mathbf{M}_d = [0.75, 0.61, 0.23]$,
 $\mathbf{M}_s = [0.63, 0.56, 0.37]$ and $n = 14$
and use the equation

$$\mathbf{I}_{gold} = (\mathbf{I} \bullet \mathbf{M}_a) + (\mathbf{I} \bullet \mathbf{M}_d) \cos \phi + (\mathbf{I} \bullet \mathbf{M}_s) \cos^n \rho,$$

where ϕ is the angle between the surface normal and the vector pointing towards the light source and ρ is the angle between the reflected light vector and the vector pointing towards the light source.

- b) Use $\mathbf{I} = [1, 1, 0]$. Otherwise do the same as in a).

Exercise 24

- a) Multipath interference (MPI) may occur when many light rays are emitted at once. MPI occur when there are multiple possible light paths from the emitter to the receiver. MPI is common in ToF cameras, when concave surfaces are observed.
Lidars normally perform scanning and has a narrow beam emitter and a narrow angle receiver, and thus only suffer from MPI from semi-transparent objects such as glass, rain, or fog. More recent Lidars can mitigate the effect further by registering multiple echoes, and selecting one.
- b) Only the Kinect v2, as the others are Lidars.